

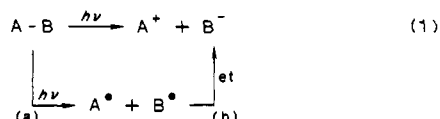
A Kinetic Study of the Photosolvolytic Cleavage of 9-Fluorenyl

Elizabeth Gaillard,[†] Marye Anne Fox,^{*,†} and Peter Wan[†]

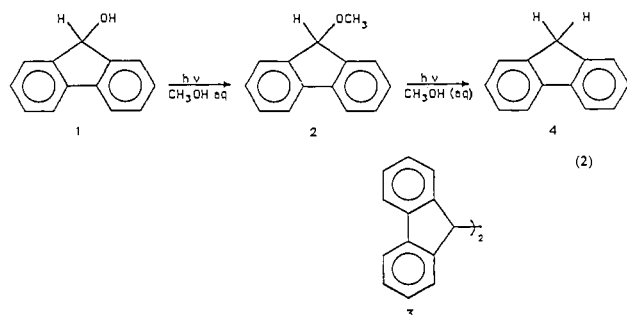
Contribution from the Department of Chemistry, University of Texas, Austin, Texas 78712, and the Department of Chemistry, University of Victoria, Victoria, British Columbia, Canada V8W 2Y2. Received June 20, 1988

Abstract: Excitation of 9-fluorenyl in methanol and methanol-water mixtures leads to both heterolytic and homolytic cleavage via the singlet excited state. The partitioning between homolysis and heterolysis is controlled by solvent composition, the rate constant for cation formation being a function of the solvent dielectric constant. The rate constants of intersystem crossing, fluorescence, and singlet-derived radical formation are linear functions of the mole fraction of water.

The possibility that photoinduced heterolytic bond cleavage, eq 1, may actually occur via homolysis (path a) and subsequent electron transfer (path b) is a fundamental question of mechanistic importance. The recent report¹ that photolysis of 9-fluorenyl (1)



in either methanol or 50% aqueous methanol leads to the formation of 9-methoxyfluorene (2) as the only observable product therefore attracted our attention. The authors postulated that 1 undergoes heterolytic bond cleavage upon excitation to yield a carbocation as the primary intermediate, which then reacts with methanol to yield the observed methyl ether, 2, eq 2. 9,9'-Bifluorene (3) and fluorene (4) were isolated after prolonged irradiation of the reaction mixture. They were thought to form by photolysis of the primary photoproduct, the methyl ether 2, via homolytic cleavage of the C-O bond (eq 2).



The rationale offered for the proposed primary heterolysis¹ is that the central ring of the fluorenyl cation can be thought of as a benzannelated $4n$ anti-Hückel cyclic system which might display aromatic properties on the excited-state surface. These conclusions concerning the photochemical reaction mechanism of 1 are unusual in two respects. First, the observed photochemistry was substantially different in 1 and 2; that is, excitation of 1 led exclusively to bond heterolysis whereas excitation of 2 proceeded mainly via homolysis. Excited-state σ bond cleavage is a common primary photochemical process, but very few of these reactions are known where only a carbocation intermediate is produced without parallel homolysis. In general, evidence for both radical and ionic intermediates has been presented.² Second, the postulated aromatic stabilization of the fluorenyl cation requires that it be formed adiabatically, which may be energetically unfavorable. Furthermore, the simple MO arguments, which predict ground-state stabilization of $4n+2$ systems (and destabilization of $4n$ systems),³ do not necessarily imply excited-state destabilization (and stabilization in $4n$ systems) of these rings, since aromatic-type stability is predicted on closed-shell electronic structures, which excited

states are unlikely to possess. The choice of an appropriate model against which to measure excited-state stabilization is not obvious.

Much of our understanding of carbocation chemistry has been inferred from product analysis. In general, direct spectroscopic characterization of carbocations in solution is difficult without the use of harsh reagents (e.g., SbCl_5 in FSO_3H).⁴ Alternatively, many of these ions can be generated photochemically, allowing for the identification of the excited state through which bond cleavage occurs and the spectroscopic characterization of any reactive intermediates observed. In order to identify the mechanism of formation of the 9-fluorenyl cation, we have reexamined this reaction via time-resolved spectroscopic techniques.

Our data indicate that excitation of the alcohol 1 in methanol and several methanol-water mixtures leads to products of both heterolytic and homolytic cleavage via the singlet excited state. Independent characterization of the fluorenyl radical and cation allows us to study the partitioning between bond homolysis and bond heterolysis as a function of solvent composition. We find the rate constant for cation formation to be a function of the solvent dielectric constant. Our data further indicate that the rate constants for the other observable deactivation processes for the singlet state, i.e., intersystem crossing, fluorescence, and radical formation, are linear functions of the mole fraction of water.

Experimental Section

9-Fluorenyl (Aldrich, 97%) was recrystallized from 50:1 (v/v) hexane-acetone and then sublimed. Xanthone (J.T. Baker), acenaphthene (Aldrich 98%), and naphthalene (MC/B) were recrystallized twice from 95% ethanol. Benzophenone (Aldrich 99%) was sublimed. *trans*-Canthaxanthin (Fluka) was used as supplied.

Methanol (Fisher Spectroanalyzed) was either distilled from sodium on a 4-ft fractionating column packed with glass helices or heated under reflux for 2 h with 2,4-dinitrophenylhydrazine (5 mg/L), before being fractionally distilled. Both methods achieved the same purity as measured by optical absorption. However, distillation from sodium was preferred in order to reduce water impurity. Acetonitrile was either used without further purification (Fisher HPLC grade) or purified by the method of Mann et al.⁵ Isooctane (Aldrich Gold Label) was passed through a 4-cm diameter column of activated silica (ca. 0.5 m/L) and only the middle fraction (ca. 40%) was collected. *tert*-Butyl alcohol (Fisher certified), carbon tetrachloride (Aldrich HPLC grade), and sulfuric acid (Fisher reagent grade) were used without further purification. Water was purified by passing through a Millipore filtration system.

9-Chlorofluorene was prepared by suspending 5 g of 9-fluorenyl in 800 mL of concentrated HCl with a catalytic amount of concentrated H_2SO_4 . The suspension was stirred for 48 h, neutralized with aqueous NaOH, and extracted with diethyl ether. After removal of the solvent, the solid material was recrystallized twice from 95% ethanol (mp 91–92 °C, lit.⁶ mp 92 °C).

(1) Wan, P.; Krogh, E. *J. Chem. Soc., Chem. Commun.* **1985**, 1207. The value for the quantum yield for methyl ether formation reported in this preliminary communication is somewhat too high (see ref 31).

(2) Cristol, S. J.; Bindel, T. H. *Org. Photochem.* **1983**, *6*, 327.

(3) Streitwieser, A.; Juarista, E.; Nebenzahl, L. L. In *Comprehensive Carbocation Chemistry*, Part A; Bunce, E., Durst, T., Eds.; Elsevier: Amsterdam, 1980; pp 323–381.

(4) Gillespie, R. J. *Acc. Chem. Res.* **1968**, *1*, 202.

(5) O'Donnell, J. F.; Ayres, J. J.; Mann, C. K. *Anal. Chem.* **1965**, *37*, 1161.

(6) Eaborn, C.; Shaw, R. A. *J. Chem. Soc.* **1954**, 2027.

[†]University of Texas.

[†]University of Victoria.

Emission/excitation spectra and fluorescence quantum yields were recorded with an SLM-Aminco SPF-500C spectrofluorometer. Fluorescence quantum yields were measured against acenaphthene in acetonitrile ($\Phi_f = 0.5$).⁷ The optical densities of all samples at the excitation wavelength 270 nm were adjusted to agree within 10% (0.40 ± 0.04). Appropriate glass filters were used at both the excitation and emission monochromators, and the highly photosensitive fluoreno samples were continuously renewed throughout the experiment.

A HP 8450 diode-array spectrophotometer was used to record absorption spectra and to monitor steady-state photolyses. The sample, contained in a 1-cm cuvette, was irradiated with a 150-W Xe lamp through a grating monochromator set at 270 nm. The cuvette was placed sufficiently far away from the exit slit of the monochromator to allow use of a narrow bandwidth and also to minimize heating of the sample. The sample was continuously stirred with a small bar magnet.

Time-resolved fluorescence data were collected via a photomultiplier tube (Hamamatsu R306, response time ca. 0.75 ns) after excitation of the sample with the frequency-quadrupled output of a mode-locked Nd:YAG laser (Quantel YG402, 200-ps pulse).

Flash-photolysis experiments were carried out with either the third or fourth harmonic of a Q-switched Nd:YAG laser for excitation (Quantel YG581, or Quantel YG481, 11-ns pulse widths). Up to 9 mJ/cm² at 355 nm and 7 mJ/cm² at 266 nm excitation pulses were used. The first millimeter of sample in the direction of the excitation pulse was analyzed. Samples were bubbled in situ with the appropriate gas or gas mixtures. The sample was changed at least every five pulses, and cutoff filters were used to protect the sample from analyzing-light photolysis.

The experimental arrangement for pulse radiolysis has been described previously.⁸ Electron pulses (100 ns, 250 ns, 50 ns, or 1 μ s) were delivered to samples contained in a quartz flow cell with a 2.4-cm optical path length. Fresh sample was injected into the cell after every pulse. Solutions were bubbled with either N₂ or O₂ prior to the experiment.

Transient absorptions were monitored with a conventional xenon lamp, monochromator, photomultiplier tube arrangement in the flash-photolysis and pulse-radiolysis experiments. Digitized signals generated in all time-resolved measurements were passed to a PDP 11/70 minicomputer for data analysis. The data analysis system has been described more fully elsewhere.⁹

Extinction coefficients and quantum yields of the transient species observed after photolysis of 9-fluoreno were measured by a comparative technique. Extinction coefficients were measured in experiments where these species are exclusively produced by either pulse radiolysis or sensitization. The absorption of the solvated electron in either methanol ($G(e^-) = 1.1$, $\epsilon_{630} = 1.73 \times 10^4 \text{ M}^{-1} \text{ cm}^{-1}$)¹⁸ or water ($G(e^-) = 2.7$, $\epsilon_{715, e^-} = 1.85 \times 10^4 \text{ M}^{-1} \text{ cm}^{-1}$)²⁵ was used as a dosimeter and xanthone ($\Phi_{isc} = 0.97$, $\lambda_{exc} = 355 \text{ nm}$)¹⁴ was used as a sensitizer. The absorption of the benzophenone triplet state, ³BP* ($\lambda_{exc} = 355 \text{ nm}$, $\lambda_{mon} = 530 \text{ nm}$, $\epsilon_{530} = 7220 \text{ M}^{-1} \text{ cm}^{-1}$, $\Phi_{isc, BP} = 1$, benzene as solvent),¹⁰ was used as an actinometer in the sensitized experiments. In all flash-photolysis experiments, sample solutions and actinometer solutions were prepared with matched optical density at the excitation wavelength. In order to measure the extinction coefficient, ϵ_λ , the absorbance of the actinometer triplet state or the dosimeter and the absorbance of the fluoreno-derived species were recorded and extrapolated to time zero for a given beam energy or dose. The concentration of the transient species produced, $[I]_{t=0}$, was calculated from the concentration of actinometer or dosimeter at time zero. Corrections were made for differences in G values, quantum yields, and scavenging efficiency when necessary. The ϵ_λ may then be calculated with Beer's law, eq 3, where OD_λ is the optical density of the

$$\epsilon_\lambda = OD_\lambda / ([I]_{t=0} l) \quad (3)$$

transient at time zero and l is the analyzed path length. The quantum yield of formation of each species, Φ , after direct excitation of **1** was measured with the naphthalene triplet state, ³Np* ($\lambda_{exc} = 266 \text{ nm}$, $\lambda_{mon} = 415 \text{ nm}$, $\epsilon_{415} = 2.45 \times 10^4 \text{ M}^{-1} \text{ cm}^{-1}$, $\Phi_{isc, Np} = 0.75$, cyclohexane as solvent),¹¹ as an actinometer (except for Φ_c ; see the Results and Discussion section). After calculation of the concentration of species pro-

Table I. Observed Emission Decay Rate Constants and Fluorescence Quantum Yields

solvent	$k_{obsd} \times 10^{-8} / \text{s}^{-1} \text{ }^a$	$\Phi_f \text{ }^b$	$k_f \times 10^{-6} / \text{s}^{-1}$
CH ₃ OH	2.0	0.03	6.0
20% aqueous CH ₃ OH	1.8	0.03	5.3
50% aqueous CH ₃ OH	1.7	0.03	5.1
90% aqueous CH ₃ OH	1.9	0.02	3.8

^aStandard errors are typically 10%. ^bAcenaphthene in acetonitrile used as a fluorescence standard ($\Phi_f = 0.5$).⁷

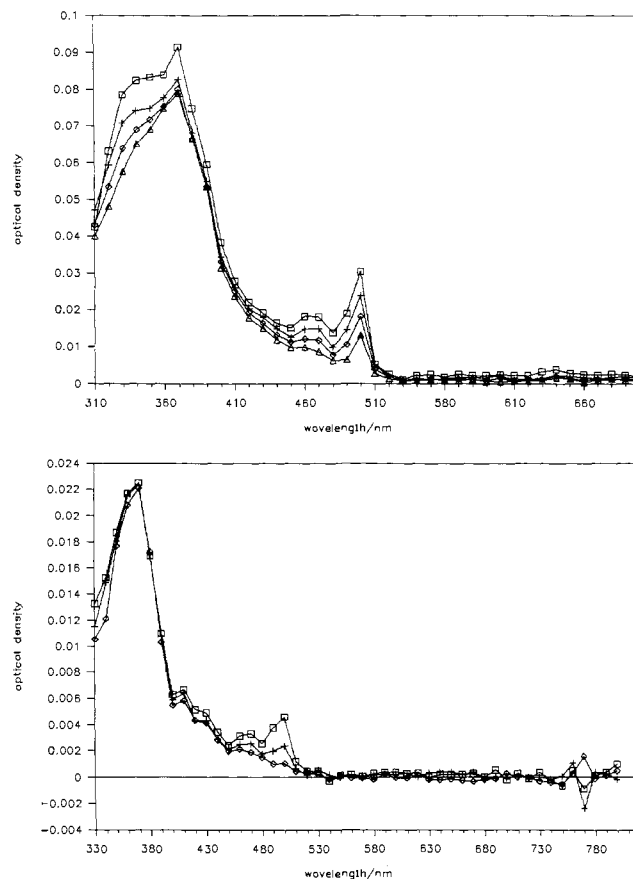


Figure 1. Absorption spectra observed at several times after excitation (266 nm, 10-ns pulse) of $1 \times 10^{-4} \text{ M}$ 9-fluoreno in N₂-saturated CH₃OH: (top) \square , 1 μ s; $+$, 3.2 μ s; \diamond , 6.5 μ s; Δ , 13.5 μ s, and (bottom) \square , 40 μ s; $+$, 130 μ s; \diamond , 1.4 ms.

duced as described above, the Φ may then be calculated from eq 4, where $[act]_{t=0}$ and Φ_{act} are the initial concentration and quantum yield of the actinometer species, respectively.

$$\Phi = ([I]_{t=0} / [act]_{t=0}) \Phi_{act} \quad (4)$$

Results and Discussion

A. Emission Measurements. The emission spectrum of **1** in methanol or a methanol-water mixture has a maximum at 325 nm (excitation into longest wavelength absorption band at 270 nm). The excitation spectrum (monitored at 325 nm) and the ground-state absorption spectrum have the same spectral features and are unperturbed by changes in solvent composition. We measured the fluorescence lifetime of **1** in methanol and three methanol-water mixtures (20%, 50%, and 90% H₂O by volume). These values are listed in Table I as observed rate constants, k_{obsd} . The fluorescence quantum yield, Φ_f , was also measured in each solvent mixture as described in the Experimental Section. The radiative rate constant, k_f , for **1** in each solvent and solvent mixture was calculated from the corresponding Φ_f and k_{obsd} values (Table I) as a product of these two values, $k_f = \Phi_f k_{obsd}$. These measurements thus appear to be unaffected by changes in solvent composition.

B. Absorption Measurements. Figure 1 shows the transient absorption spectrum observed upon photolysis of **1** in N₂-saturated

(7) Birks, J. B. In *Photophysics of Aromatic Molecules*; Wiley: New York, 1970; p 70.

(8) Rodgers, M. A. J.; Foyt, D. C.; Zimek, Z. A. *Radiat. Res.* **1977**, *75*, 296.

(9) Foyt, D. C. *Comput. Chem.* **1981**, *5*, 49.

(10) Hurley, J. K.; Sinai, N.; Linschitz, H. *Photochem. Photobiol.* **1983**, *38*, 9.

(11) The actinometer used for simultaneous irradiation with the solutions of varying solvent composition was always naphthalene in cyclohexane: Bensasson, R.; Land, E. J. *Trans. Faraday Soc.* **1971**, *67*, 1904 (extinction coefficient). Amand, B.; Bensasson, R. *Chem. Phys. Lett.* **1975**, *34*, 44 (quantum yield).

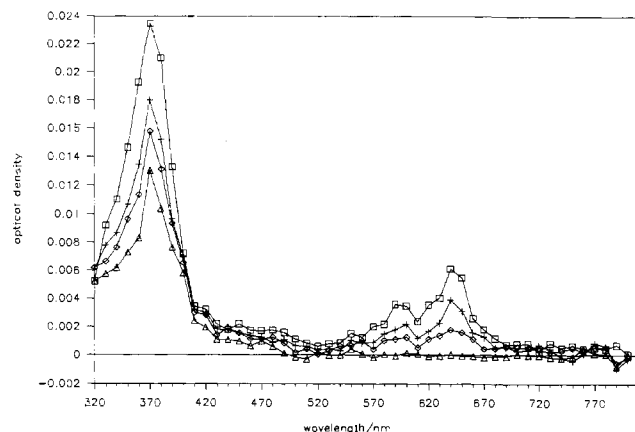


Figure 2. Absorption spectra observed at several times after excitation (266 nm, 10-ns pulse) of 5×10^{-4} M 9-fluorenone in air-saturated 90% (v/v) aqueous CH_3OH ; \square , 2 μs ; $+$, 5 μs ; \diamond , 8.5 μs ; Δ , 67.3 μs .

methanol at several times after the pulse (266 nm, 10-ns pulse width). There are at least two transient species, **5** and **6**, which we assign (see below) to the triplet excited state **5** ($\lambda_{\text{max}} = 370$ nm) and the free radical **6** ($\lambda_{\text{max}} = 500$ nm), respectively, and a residual absorption, **9**, stable over 40 ms, the longest time scale monitored. A third transient species, **7**, which we assign (see below) to the cation ($\lambda_{\text{max}} = 640$ nm), appears when water is added to the solvent, along with a decrease in the absorption at 500 nm (Figure 2). (Air saturation has the effect of removing spectral contributions from T-T absorption and from the triplet **5**.) These assignments are derived from experimental observations when **1** is directly excited in methanol and aqueous methanol and when each of the transient species is produced independently.

The triplet decays via first-order kinetics with a rate constant that is dependent on the ground-state concentration. A plot of this first-order rate constant as a function of ground-state concentration gives a bimolecular rate constant of $1.2 \times 10^7 \text{ M}^{-1} \text{ s}^{-1}$ for reaction of **5** with the ground state and a lifetime of 15 μs extrapolated to zero concentration. Measurement of the rate constant for decay of **5** as a function of oxygen concentration ($[\text{O}_2]_{\text{max}}$ in $\text{CH}_3\text{CN} = 8.6 \times 10^{-3} \text{ M}$)¹² leads to a bimolecular rate constant of $3.2 \times 10^9 \text{ M}^{-1} \text{ s}^{-1}$ for quenching by oxygen.

The free radical **6** decays via second-order kinetics ($k/\epsilon l = 4.1 \times 10^6 \text{ s}^{-1}$), independent of the ground-state concentration. In the presence of oxygen, **6** decays exponentially. Measurement of the rate constant as a function of oxygen concentration ($[\text{O}_2]_{\text{max}}$ in $\text{CH}_3\text{OH} = 1.01 \times 10^{-2} \text{ M}$)¹³ gives a bimolecular rate constant of $1.9 \times 10^8 \text{ M}^{-1} \text{ s}^{-1}$ for its reaction with oxygen.

The intensity of the transient absorption attributable to the cation **7** increases with increasing water concentration. This species **7** decays via first-order kinetics ($1.6 \times 10^5 \text{ s}^{-1}$ in 90% aqueous methanol). This rate constant varies only slightly with solvent composition but is insensitive to oxygen. This solvent insensitivity suggests that capture of **7** by water occurs with comparable facility to that by methanol, providing an additional route for recovery of starting material.³⁰

C. Fluorenone Triplet 5. Formation of **5** can be sensitized by energy transfer from the $\pi\text{-}\pi^*$ triplet state of xanthone, $^3\text{X}^*$ ($E_{\text{T}} = 69 \text{ kcal/mol}$ in polar solvents¹⁴). Excitation of xanthone in the presence of **1** (10^{-1} M) leads to complete quenching of the $^3\text{X}^*$ signal and to the appearance of an absorption at 370 nm. Figure 3 shows the observed transient absorption spectrum at several different times after the pulse (355 nm, 10-ns pulse

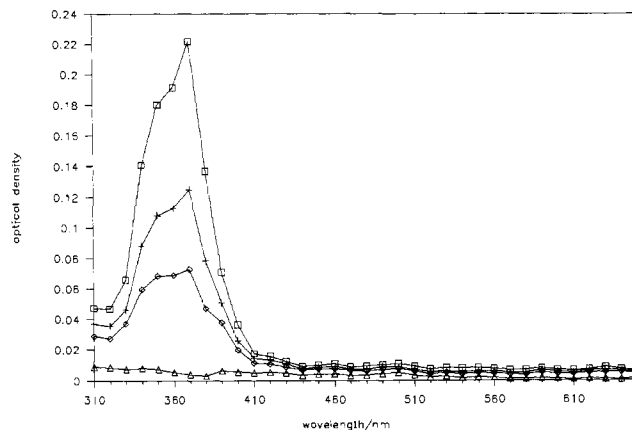


Figure 3. Absorption spectra attributed to the 9-fluorenone triplet state **5** produced via sensitization at several times after excitation (355 nm, 10-ns pulse) of 1×10^{-4} M xanthone and 5×10^{-3} M 9-fluorenone in N_2 -saturated CH_3CN ; \square , 1 μs ; $+$, 2.5 μs ; \diamond , 4.3 μs ; Δ , 33.6 μs .

Table II. Intersystem Crossing Quantum Yields and Rate Constants

solvent	$\Phi_{\text{isc}} \times 10^2$ ^{a,b}	$k_{\text{isc}} \times 10^{-6}/\text{s}^{-1}$
CH_3OH	3.4	6.8
20% aqueous CH_3OH	2.0	3.6
50% aqueous CH_3OH	1.7	2.9
90% aqueous CH_3OH	0.8	1.5

^aNaphthalene triplet-triplet absorption used as an actinometer.¹¹
^b ϵ_{370} assumed to be solvent independent; standard errors vary from 18% to 22%.

width).¹³ An important observation is that the entire spectrum decays back to the prepulse base line, indicating that triplet **5** does not lead to any new absorbing species. The rate constants for decay of $^3\text{X}^*$ at 630 nm and the growth of triplet fluorenone **5** at 370 nm were identical within experimental error [$(1.0 \pm 0.1) \times 10^7 \text{ s}^{-1}$] for a sample with $7 \times 10^{-4} \text{ M}$ **1**. The decay at 370 nm was monitored for a solution of xanthone and **1** ($1 \times 10^{-1} \text{ M}$) in acetonitrile that was either air-, N_2 -, or O_2 -saturated. A plot of the first order decay rate constant at 370 nm vs $[\text{O}_2]$ affords a quenching rate constant of $3.5 \times 10^9 \text{ M}^{-1} \text{ s}^{-1}$, similar to that observed when the alcohol **1** is excited directly.

We also observed sensitization of the *trans*-canthaxanthin triplet state, $^3\text{C}^*$ ($E_{\text{T}} = 23 \text{ kcal/mol}$),¹⁵ by triplet **5**. The enhanced decay at 370 nm and the concomitant growth of the *trans*-canthaxanthin triplet-triplet absorption at 560 nm¹⁵ were monitored in experiments where **5** was produced by sensitization ($1 \times 10^{-4} \text{ M}$ xanthone, $4 \times 10^{-2} \text{ M}$ **1**, and $2 \times 10^{-4} \text{ M}$ *trans*-canthaxanthin) or by direct excitation of **1** ($4 \times 10^{-5} \text{ M}$ **1** and $2 \times 10^{-4} \text{ M}$ *trans*-canthaxanthin). The observed rate constants for the decay of **5** are 9.7×10^5 and $6.0 \times 10^5 \text{ s}^{-1}$ and for the growth of $^3\text{C}^*$ at 560 nm are 7.6×10^5 and $5.8 \times 10^5 \text{ s}^{-1}$ for the sensitized and direct experiments, respectively. The rate constants in the sensitized experiment are larger than those for direct excitation (for the same concentration of quencher) because of the larger contribution from self-quenching, $k_{\text{sq}}[\text{I}]$, to the observed decay rate constant. We also observe that the rate constant for decay of **5** formed via sensitization ($k_{\text{sq}} = 9.6 \times 10^6 \text{ M}^{-1} \text{ s}^{-1}$) has the same dependence on the concentration of **1** as that formed by direct excitation ($k_{\text{sq}} = 1.2 \times 10^7 \text{ M}^{-1} \text{ s}^{-1}$).

In order to measure the quantum yield of intersystem crossing, Φ_{isc} , as a function of solvent composition, we first measured the extinction coefficient of the triplet **5** at 370 nm (ϵ_{370}). We assumed that ϵ_{370} is independent of solvent and, for experimental simplicity, made measurements in CH_3CN . Xanthone was used to sensitize **5**, with known quantum yield, and to eliminate complications from other absorbing species. Since **1** scavenges $^3\text{X}^*$ with a bimolecular rate constant of $1.5 \times 10^{10} \text{ M}^{-1} \text{ s}^{-1}$ and $^3\text{X}^*$ naturally decays with a first order rate constant of $1.2 \times 10^5 \text{ s}^{-1}$, then $3 \times 10^{-3} \text{ M}$ **1** will scavenge approximately 99.7% of $^3\text{X}^*$. The ϵ_{370} was measured

(12) For the oxygen solubility in acetonitrile, see: Smothers, W. K.; Meyer, M. C.; Saltiel, J. S. *J. Am. Chem. Soc.* **1983**, *105*, 545. For the oxygen solubility in methanol, see: *Solubilities. Inorganic and Metal-Organic Compounds*, 4th ed.; Linke, W. F., Ed.; American Chemical Society: Washington, DC, 1965; Vol. II, p 1235.

(13) The shifts in T-T absorption maxima in Figures 1 and 3 probably derives from solvent sensitivity of such spectra (Hug, G. L.; Carmichael, I. *J. Phys. Chem. Ref. Data* **1986**, *15*, 1).

(14) Scaiano, J. C. *J. Am. Chem. Soc.* **1980**, *102*, 7747.

(15) Rodgers, M. A. J.; Bates, A. L. *Photochem. Photobiol.* **1980**, *31*, 533.

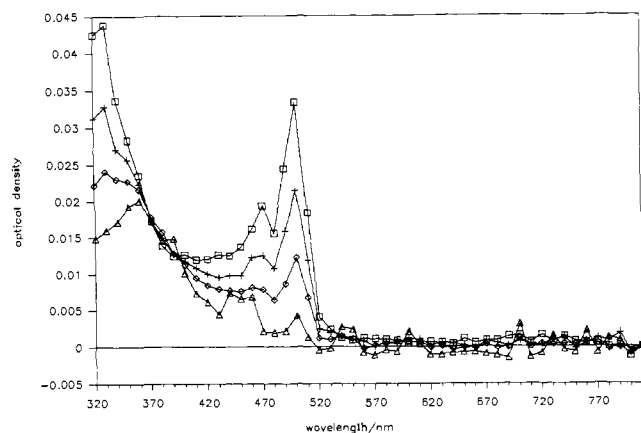
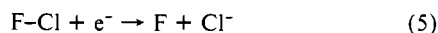


Figure 4. Absorption spectra attributed to 9-fluorenyl free radical **6** produced via pulse radiolysis of 6×10^{-3} M 9-chlorofluorene and 0.4 M *tert*-butyl alcohol in N_2 -saturated CH_3OH . The spectra were recorded at the following times after a 500-ns pulse: \square , 2 μ s; $+$, 14 μ s; \diamond , 44 μ s; Δ , 270 μ s.

with the benzophenone triplet state, $^3BP^*$, as an actinometer.¹⁰ The optical density at time zero of **5** was corrected for the quantum yield of intersystem crossing of xanthone before applying eq 2. The ϵ_{370} [$(2.1 \pm 0.2) \times 10^4 M^{-1} cm^{-1}$] was found to be independent of laser intensity.

The quantum yield of intersystem crossing, Φ_{isc} , for **1** as a function of solvent was measured with the naphthalene triplet state, $^3Np^*$, as an actinometer.¹¹ The Φ_{isc} values calculated from eq 4 are found in Table II.¹⁶

D. Fluorenyl Radical 6. The transient absorption observed at 500 nm is assigned to the fluorenyl radical **6**. This assignment is based on previously reported spectra¹⁹ and independent production of **6** in methanol via pulse radiolysis. The radiation chemistry of methanol is well characterized.¹⁷ The primary species are electrons ($G(e^-) = 1.1$, $\epsilon_{630} = 1.73 \times 10^4 M^{-1} cm^{-1}$),¹⁸ several neutral free radicals (e.g., CH_3O^\bullet , $^\bullet CH_2OH$, $^\bullet OH$), and various stable products. The addition of *tert*-butyl alcohol (2% by volume) results in the conversion of the initially formed radicals to the relatively unreactive *tert*-butyl alcohol radical. Pulse radiolysis of a N_2 -saturated solution of 9-chlorofluorene (**8**) (6×10^{-3} M) in methanol with 2% *tert*-butyl alcohol results in the formation of **6** via dissociative electron capture (eq 5). The resulting transient absorption spectrum (Figure 4) is similar to that observed after photolysis of **1** in methanol.



The decay of **6** is best fit via a second-order rate expression with an observed rate constant [$k_{dr}/\epsilon_{500}l = (1.7 \pm 0.1) \times 10^6 s^{-1}$] that is independent of dose. The extinction coefficient of **6** at 500 nm (ϵ_{500}) was measured relative to the absorption of the electron in methanol as a dosimeter. We observe that the chloride **8** reacts with the electron with a bimolecular rate constant of approximately $1 \times 10^{10} M^{-1} s^{-1}$ and that the electron decays with a rate constant of $6.5 \times 10^5 s^{-1}$ in purified methanol. Therefore, we assume that $G(\mathbf{6})$ is equal to $G(e^-)$ for a solution of 6×10^{-3} M **8**. The ϵ_{500} [$(3.6 \pm 0.3) \times 10^3 M^{-1} cm^{-1}$] was found to be independent of dose. With this value of ϵ_{500} , the bimolecular decay rate constant, k_{dr} , of **6** can be calculated from the observed decay rate constant at 500 nm. Identical values, within experimental error [(1.5 ± 0.5)

(16) Because the absorption spectrum of the triplet **5** decays to zero under sensitized conditions, we are confident that the decay of **5**, produced via direct excitation of **1**, does not lead to any new absorption at 370 nm. We therefore assume that any contribution to the absorption at 370 nm from **6** or **7** (the transients observed at 500 nm and 640 nm in Figures 1 and 2) were also present at the same time as **5**. Thus, we measured the time-zero contribution of triplet **5** at 370 nm by fitting only the initial portion of the decay.

(17) Tepley, J. *Radiat. Res.* **1969**, *1*, 361.

(18) Sauer, M. C.; Aral, S.; Dorfman, L. M. *J. Chem. Phys.* **1965**, *42*, 708.

(19) Norman, I.; Porter, G. *Proc. Ro. Soc. London, A* **1955**, *230A*, 399.
Wong, P. C.; Griller, D.; Scaiano, J. C. *J. Am. Chem. Soc.* **1981**, *103*, 5934.
Grasse, P. B.; Brauer, B.; Zupancic, J. J.; Kaufmann, K. J.; Schuster, G. B. *J. Am. Chem. Soc.* **1983**, *105*, 6833.

Table III. Free Radical Quantum Yields and Formation Rate Constants

solvent	$\Phi_{fr}^{a,b}$	$k_{fr} \times 10^{-6}/s^{-1}$
CH_3OH	0.12	24
20% aqueous CH_3OH	0.08	14
50% aqueous CH_3OH	0.05	8.8
90% aqueous CH_3OH	0.03	5.5

^a Naphthalene triplet-triplet absorption used as an actinometer.¹¹
^b ϵ_{500} assumed to be solvent independent; standard errors vary from 15% to 20%.

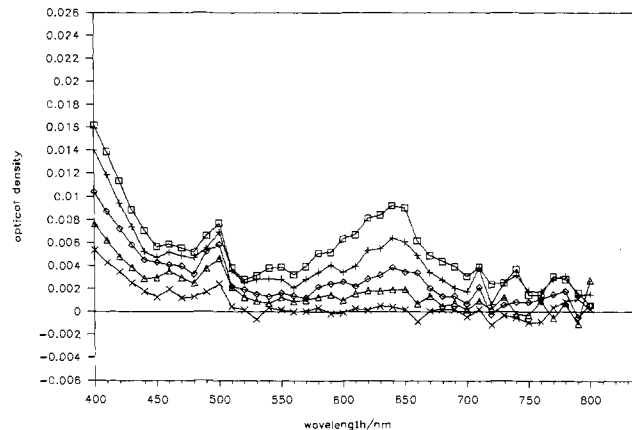


Figure 5. Absorption spectra attributed to the 9-fluorenyl carbocation **7** produced via pulse radiolysis of 1×10^{-3} M 9-chlorofluorene and 1×10^{-2} M CCl_4 in N_2 -saturated isooctane. The spectra are for the following times after a 250-ns pulse: \square , 800 ns; $+$, 1.4 μ s; \diamond , 2.6 μ s; Δ , 5.4 μ s; \times , 26.9 μ s.

$\times 10^{10} M^{-1} s^{-1}$], are obtained from both the pulse-radiolysis and flash-photolysis data.

Quantum yields of radical formation, Φ_{fr} , from direct photolysis of the parent alcohol **1** in several solvent mixtures are reported in Table III. $^3Np^*$ was used as an actinometer. If we assume that **6** is produced directly from the singlet excited state of **1**, then we can calculate k_{fr} , the rate constant of radical formation, as a product of Φ_{fr} and k_{obsd} . This assumption is based on two observations: first, that triplet **5** did not lead to absorptions characteristic of **6** in sensitized experiments, and second, that the absorption at 500 nm occurs within the duration of the pulse (266 nm, 10 ns) in the flash-photolysis experiments. Values of k_{fr} are also presented in Table III.

E. Fluorenyl Cation 7. The transient absorption observed at 640 nm upon addition of water is assigned to the fluorenyl carbocation **7**. Formation of **7** has been proposed to explain the blue color of dilute solutions of the alcohol **1** in concentrated sulfuric acid.²⁰ We also observe that dilute solutions of **1** in concentrated H_2SO_4 are blue, with absorption maxima at 480 and 660 nm. We prefer to produce **7** by pulse-radiolytic methods because this route allows us to obtain kinetic as well as spectral information. In addition, these techniques allow us to selectively generate **7** in a chemical environment that is more comparable to that involved in flash photolysis in methanol.

Several studies of organic radical cations and carbocations produced via radiolysis in hydrocarbon^{21,23} and chloroalkane²² solvents have been reported. For example, Allen and Capellos²³ have measured the yield of free ions (G_f) in several organic solvents via charge scavenging with triphenylmethyl chloride (TPMC). They obtained results in excellent agreement with values measured by the clearing-field method.²⁴ Absorptions assigned to both the triphenylmethyl free radical and carbocation were observed after

(20) Lifschitz, I. *Recl. Trav. Chim. Pays-Bas* **1935**, *54*, 397.

(21) Keene, J. P.; Land, E. J.; Swallow, A. J. *J. Am. Chem. Soc.* **1965**, *87*, 5284.

(22) Dorfman, L. M. In *Fast Reactions in Energetic Systems*; Capellos, C., Walker, R. F., Eds.; D. Reidel Publishing Co.: London, 1981; p 95.

(23) Capellos, C.; Allen, A. O. *J. Phys. Chem.* **1969**, *73*, 3264.

(24) Schmidt, W. F.; Allen, A. O. *Science* **1968**, *160*, 300.

Table IV. Cation Quantum Yields and Formation Rate Constants

solvent	$\Phi_c \times 10^2$ ^{a,b}	$k_c \times 10^{-6}/s^{-1}$
CH ₃ OH	0.3	0.6
20% aqueous CH ₃ OH	0.7	1.3
50% aqueous CH ₃ OH	2.8	4.8
90% aqueous CH ₃ OH	3.9	7.5

^a Visible absorption of **6** used as an actinometer. ^b ϵ_{640} assumed to be solvent independent; standard errors vary from 27% to 31%.

irradiation of TPMC in N₂-saturated isooctane. It was proposed that the radical and cation were formed from TPMC by dissociative electron capture and reaction with the solvent positive ion, respectively. The yield of radical was observed to increase with increasing alkyl halide concentration, the yield in excess of G_{fi} being attributed to recombination of geminate electron-carbocation pairs in the spur. The yield of cation was observed to be independent of alkyl halide concentration and equal to the total yield of free ions in isooctane ($G_{fi} = 0.34$).^{23,24} Several years later, Zador et al.²⁵ confirmed the production of both species in the pulse radiolysis of cyclohexane solutions of TPMC as well as the formation of the free radical by dissociative electron capture. However, they observed that reaction of TPMC with the solvent positive ion resulted in formation of the TPMC radical cation, which decayed over several hundred nanoseconds to yield the cation. Figure 5 shows the spectrum observed after pulse radiolysis of **8** (10^{-3} M) in N₂-saturated isooctane containing 0.01 M CCl₄.²⁶ Assuming that reactions analogous to those observed for TPMC occur for chloride **8**, this spectrum is attributed to the cation **7**. No increase in the cation absorption near the end of pulse is detected. Because the shortest pulse width used in these experiments is 250 ns, we do not exclude the 9-chlorofluorene radical cation as a precursor to **7**. The decay of **7** follows second-order kinetics, $k/\epsilon_{640}l = 1.1 \times 10^8 s^{-1}$, in contrast to the decay in methanol-water mixtures, which exhibits first-order kinetics. We note that the absorption maximum of **7** is considerably red-shifted compared with that of **6**.

The extinction coefficient of **7** at 640 nm (ϵ_{640})²⁷ was measured with the absorption of the electron in water as a dosimeter. From the values $G(e^-) = 2.7$ and $\epsilon_{715,e^-} = 1.85 \times 10^4 M^{-1} cm^{-1}$,²⁸ we may calculate the concentration of cation **7** formed under equivalent-dose conditions.²⁷ By extrapolation of the absorbance of **7** to time zero via second-order kinetics, we calculate an extinction coefficient of $(4.2 \pm 0.4) \times 10^3 M^{-1} cm^{-1}$ for **7** at 640 nm. From ϵ_{640} and the observed decay rate constant, we obtain a value of $1.2 \times 10^{12} M^{-1} s^{-1}$ for the bimolecular decay rate constant of **7**, k_{dc} . Although our kinetic measurements do not allow correlation of transient decay with the appearance of a specific stable product, this value of k_{dc} is typical for diffusion-controlled recombination of oppositely charged species in a highly nonpolar solvent.²⁹

Quantum yields of cation formation, Φ_c , as a function of solvent were measured with the absorption of the radical **6**, produced via flash photolysis of **1** in methanol, as an actinometer. We chose **6** as an actinometer for the following reasons. In order to obtain reproducible values of the optical density at 640 nm, it was

(25) Zador, E.; Warman, J. M.; Hummel, A. *J. Chem. Soc., Faraday Trans. 1* **1979**, *75*, 914.

(26) In order to remove the radical **6** as an absorbing species, we added CCl₄ to react with the electron. The rate constant reported in the literature for this reaction is $8.9 \times 10^{12} M^{-1} s^{-1}$. (Baxendale, J. H.; Geelen, B. P. H. M.; Sharpe, P. H. G. *Int. J. Radiat. Phys. Chem.* **1976**, *8*, 371.)

(27) Correction has been made for the differing electron densities of isooctane and water. The yield of **7** is assumed to be equal to G_{fi} in these experiments for the following reasons. First, the electron-cation recombination reaction postulated by Allen and Capellos takes place in the spur and is therefore independent of free-ion scavenging. Second, because CCl₄ reacts with the electron in isooctane with a rate constant of $8.9 \times 10^{12} M^{-1} s^{-1}$ and the rate of recombination of geminate ions in isooctane is approximately $10^{12} s^{-1}$, the addition of 10^{-2} M CCl₄ should not have a significant effect on G_{fi} .

(28) Hart, E. J.; Anbar, M. *The Hydrated Electron*; Wiley: New York, 1970; p 40.

(29) Warman, J. M. In *The Study of Fast Processes and Transient Species by Electron Pulse Radiolysis*; Baxendale, J. H., Busi, F., Eds.; D. Reidel: Dordrecht, 1982; p 433.

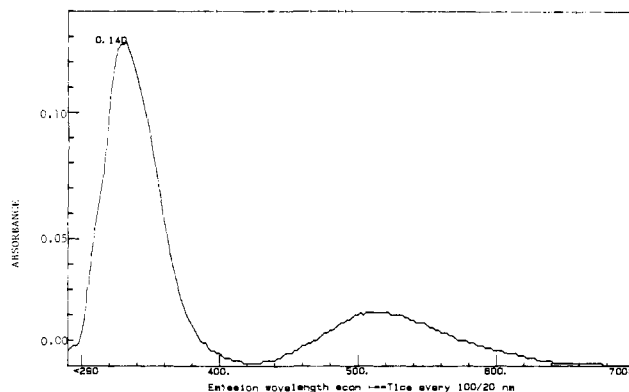


Figure 6. Emission spectrum observed after brief irradiation (260 nm) of 1×10^{-5} M 9-fluorenyl in CH₃OH ($OD_{260nm} = 0.12$).

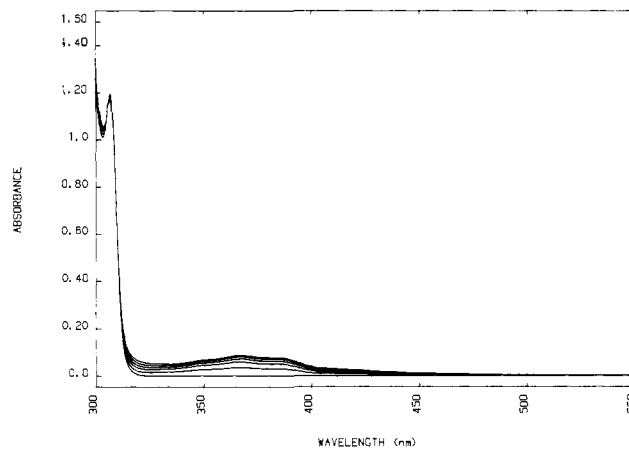


Figure 7. Absorption spectral changes observed during the steady-state photolysis of 5×10^{-4} M 9-fluorenyl in N₂-saturated CH₃OH ($OD_{270nm} > 3$ where $\lambda_{exc} = 270$ nm).

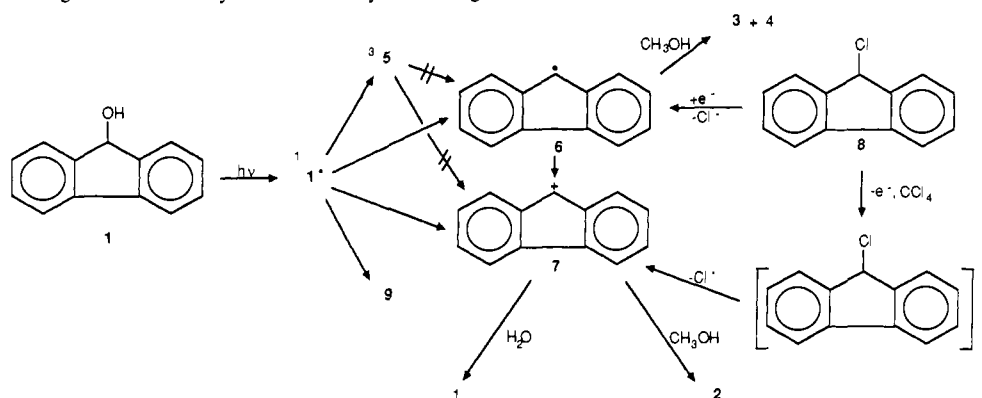
necessary to employ the maximum laser energy (7 mJ/cm² at 266 nm). Under these conditions, we observe photoionization of naphthalene, whereas **1** appears to undergo only monophotonic absorption.³⁰ Our calculated values of Φ_c and k_c , the intrinsic rate constant for cation formation, are listed in Table IV.³¹

F. Metastable Photoproduct 9. The long-lived species **9** has not been unambiguously identified. The difference absorption spectrum of **9** (Figure 1, 1.4 ms after the pulse) extends beyond 400 nm. None of the reported photoproducts (**2-4**) absorb in this region. The species **9** is formed in both CH₃OH and CH₃CN solutions, and we observe no significant change in the residual optical density produced in O₂- or N₂-saturated samples. However, the yield of **9** decreases with increasing water concentration. The

(30) This assumption is based on the following experimental observations. The time-zero optical densities of the triplet **5**, the radical **6**, and the cation **7** and the residual optical density attributed to species **9** decrease linearly as the beam energy is attenuated. We do not observe the characteristic absorption of the solvated electron in any of these solvent mixtures nor any changes in the transient absorption spectrum for samples that are saturated with N₂O. At the low conversions observed in our experiments, insufficient methyl ether is formed to complicate product analysis. Our results therefore do not provide information concerning possible cation formation from the steady-state photolysis of **2**.

(31) The values of k_c are calculated with the expression $k_c = \Phi_c k_{obsd}$ assuming that **7** is formed directly from the singlet excited state of the parent alcohol **1**. We base the validity of these calculations on arguments similar to those used for k_{tr} . The calculated values for the quantum yields of solvated cation as listed in Table IV are lower than those reported for methyl ether formation under steady-state illumination (ref 1). A redetermination of this latter quantum yield by one of us (P.W.) has shown that the originally reported value¹ was too high and should be revised downward to about 0.15. Even with large error limits in the values in Table IV caused by uncertainties in the calculation of the extinction coefficient for **7** and with reasonable experimental uncertainty for the steady-state quantum yield, these values appear to differ. One would expect these quantum efficiencies to be equal, however, only if methyl ether formation derives solely from solvated ground-state cation.

Scheme I. Partitioning between Homolytic and Heterolytic Cleavage in Photoexcited 9-Fluorenone



rate of formation of **9** cannot be measured directly in our time-resolved experiments because of overlapping transient absorptions in the accessible spectral region.

The steady-state photolysis of the alcohol **1** in N_2 -saturated methanol could be followed by emission (Figure 6) or optical-absorption (Figure 7) spectroscopy. Prior to irradiation, the excitation spectrum monitored at the emission maximum (325 nm) of **1** is identical with its ground-state absorption spectrum. Irradiation at 270 nm causes the absorption bands of **1** at 230 nm and 270 nm to decrease and new absorptions to appear (260 nm and a broad, structured band between 320 nm and 500 nm), Figure 7. Isosbestic points are observed at 240, 265, and 285 nm. Photolysis also causes the intensity of the emission at 325 nm to increase and a new emission appears (510 nm). This band is not observed in the emission spectra of any of the reported products **2**–**4**. Upon prolonged irradiation, the visible absorption and the emission at 510 nm decrease while the absorption at 260 nm and the emission at 325 nm continue to increase. If the solution is placed in the dark after a short irradiation time, the loss of the long-wavelength absorption occurs approximately 3 times more slowly than if photolysis is continued. Attempts to characterize this species by monitoring changes in the IR and 1H NMR spectra during photolysis have been inconclusive, but the appearance of signals in the region for vinylic protons in the NMR spectrum is suggestive of a photorearrangement. A logical possibility for its formation might involve a photoinduced [1,3]-sigmatropic shift of the OH group,³² giving a rearranged product capable of reversion to starting material through either a photochemical [1,3]-shift or a sequence of thermal [1,5]-sigmatropic bond migrations.

G. Mechanism. Upon 266-nm photolysis of **1** in methanol and methanol–water mixtures, we observe transient absorptions assigned as the triplet excited state **5**, the free radical **6**, the carbocation **7**, and a residual absorption from an unidentified species **9** (Scheme I). It is clear that the excited-state chemistry is more complex than suggested by previously reported product-isolation studies.¹

The formation of **6** or **7** from the triplet **5** has been discounted since the absorptions assigned to **6** and **7** appear immediately upon excitation (266 nm, 10-ns pulse) with no further increase of ab-

sorption on the time scale of triplet decay.³³ Furthermore, **5** formed via sensitization decays directly to the prepulse base line with no concomitant growth of product absorption, and the yields of **6** and **7** are largely unaffected by the presence of O_2 . In contrast, **5** is efficiently quenched by O_2 at a rate approaching diffusion control. Thus, we conclude that both **6** and **7** are derived from the excited singlet state and that the decay of the triplet state leads only to repopulation of the ground state with no product formation.

The addition of water to the solvent has a pronounced effect on the transient absorption spectrum (Figure 3). The absorptions assigned to **7** increase significantly while those assigned to **5** and **6** are diminished. These changes are reflected in the calculated rate constants for fluorescence (k_f) and for formation of **5** (k_{isc}), **6** (k_{rf}), and **7** (k_c), (Tables I–IV). The rate constants k_{isc} , k_{rf} , and k_f all decrease linearly with the increasing mole fraction of water but not with the concentration of water. This indicates that water affects the decay of the singlet excited state **1** through a bulk-solvent property and does not appear in the rate expression for the photochemical reaction.

The increase in k_c upon addition of water is not linear with either the mole fraction or the concentration of water. Instead, k_c increases linearly with the reciprocal of the solvent dielectric constant, which ranges from 33 for pure methanol to 74 for 90% aqueous methanol. This behavior is predicted by the Born equation, which relates the free energy of ion formation with the electrical work involved in transferring an ion from a vacuum to a medium of dielectric constant D .^{34,35}

According to transition-state theory, the natural logarithm of k_c , the rate constant for cation formation, is proportional to the free energy of cation formation. We have plotted our values of $\ln k_c$ versus $(D - 1/D)$, (Figure 9) and find relatively good linearity.

The decrease in the yield of free radical with increasing water content is probably a viscosity effect. Koenig et al.³⁶ have derived

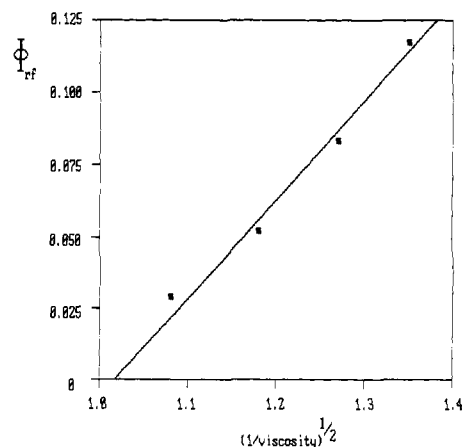


Figure 8. Dependence of the quantum yield of cage escape, Φ_{rf} , for the fluorenyl radical on solvent viscosity, η .

(32) Dormans, G. J. M.; Fransen, H. R.; Buck, H. M. *J. Am. Chem. Soc.* **1984**, *106*, 1213.

(33) We followed the growth of absorption at the visible maxima of **6** and **7** (500 nm and 640 nm, respectively) in experiments with increased time resolution (ca. 1-ns PMT rise time, 200-ps excitation pulse). The observed rate constant for growth at both 500 nm and 640 nm is $2 \times 10^8 \text{ s}^{-1}$. These values are much greater than the decay of the triplet **5** (ca. $6 \times 10^4 \text{ s}^{-1}$ for similar [1]) and are nearly identical with the observed rate constant for emission ($k_{obsd} = 2.0 \times 10^8 \text{ s}^{-1}$, in methanol).

(34) Holjtinik, G. J.; De Boer, E.; van der Meij, P. H.; Wujland, W. P. *Recl. Trav. Chim. Pays-Bas* **1956**, *75*, 487.

(35) Fischer-Hjalmars, I.; Henriksson-Enflo, A.; Herrmann, C. *Chem. Phys.* **1977**, *24*, 167.

(36) Koenig, T.; Deinzer, M. *J. Am. Chem. Soc.* **1968**, *90*, 7014. Koenig, T.; Cruthoff, R. *Ibid.* **1969**, *91*, 2562. Koenig, T.; Huntington, J.; Cruthoff, R. *Ibid.* **1970**, *92*, 5413.

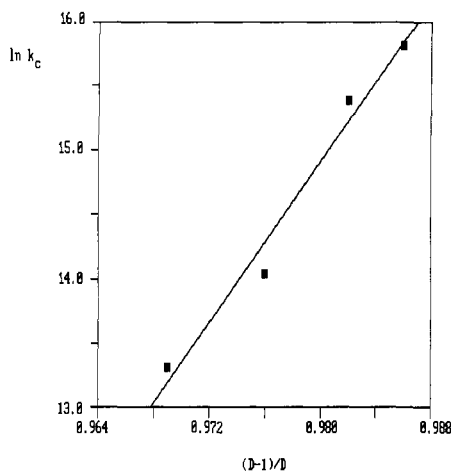


Figure 9. Dependence of the rate constant for cation formation, k_c , on solvent dielectric constant, D , as predicted by the Born equation.

equations based on the theory of Brownian motion predicting a linear relationship between the quantum yield of cage escape, Φ_{rf} , and the square root of inverse solvent viscosity, $(1/\eta)^{1/2}$. Figure 8 shows our data plotted accordingly. Even though the points show some upward curvature, they are within the error limits of the "best fit" straight line.

H. Conclusions. Photolysis of 9-fluorene in methanol or aqueous methanol leads to the production of the fluorenyl radical as well as the fluorenyl cation. Both of these species are formed via the singlet excited state of 9-fluorene. The partitioning between C-O bond homolysis and heterolysis is controlled by the

medium dielectric. The rate constant for cation formation increases as the solvent dielectric constant increases as predicted by the Born equation. Thus, we conclude that the increase in yield of the fluorenyl cation with increasing amounts of water in the solvent mixture can be attributed to a lowering of the free energy necessary for ion solvation as the solvent becomes more polar.

The possibility of cation formation via electron transfer in the geminate radical pair cannot be ruled out. The oxidation potential of the fluorenyl radical in acetonitrile and the redox potential of OH/OH^- at $\text{pH} = 7$ are reported to have values of +0.52 mV vs NHE³⁷ and +1.89 V vs NHE,³⁸ respectively. Given these values, it is thermodynamically possible for electron transfer to occur. However, the observed rate constant for radical and cation production requires the sum of the decay rate constants for the geminate radical pair to be equal to or greater than that observed for the decay of the fluorene singlet excited state.

Acknowledgment. This work was supported by the National Science Foundation (at the University of Texas) and by the Natural Sciences and Engineering Research Council of Canada (at the University of Victoria). The flash-photolysis and pulse-radiolysis experiments were conducted at the Center for Fast Kinetics Research, which is jointly supported by the National Institute of Health (RR00886-13) and by the University of Texas. We thank B. K. Naumann for assistance in the pulse-radiolysis experiments and Dr. M. A. J. Rodgers for a sample of *trans*-canthaxanthin.

Registry No. 1, 1689-64-1; 6, 2299-68-5; 7, 34985-70-1; 8, 6630-65-5.

(37) Wagner, D. D. M.; McPhee, D. J.; Griller, D. *J. Am. Chem. Soc.* **1988**, *110*, 132.

(38) Schwarz, H. A.; Dodson, R. W. *J. Phys. Chem.* **1984**, *88*, 3643.

Kinetic and Spectroscopic Studies on the Thermal Decomposition of 2,2,6-Trimethyl-4*H*-1,3-dioxin-4-one: Generation of Acetylketene¹

Robert J. Clemens* and J. Stewart Witzeman*

Contribution from the Eastman Chemicals Division Research Laboratories, Eastman Kodak Company, P.O. Box 1972, Kingsport, Tennessee 37662. Received August 19, 1988

Abstract: Acetylketene is shown to be a reactive intermediate in thermolytic reactions of 2,2,6-trimethyl-4*H*-1,3-dioxin-4-one (the diketene-acetone adduct) via a series of kinetic studies. The uncatalyzed acetoacetylations of phenol, 1-butanol, and di-*n*-butylamine with the title dioxinone at 82–107 °C are first-order reactions in which the rate-limiting step is the formation of acetylketene and acetone, presumably via a retro-Diels-Alder reaction. Isopropenyl acetoacetate is not an intermediate in the aforementioned reactions but also provides acetylketene when heated. Acetylketene was observed by FT-IR spectroscopy in an argon matrix.

Acetylketene has been of interest since the beginning of this century, but its existence has not yet been rigorously established. Diketene was long believed to be acetylketene, and once the correct structure of diketene was established, acetylketene continued to be proposed as an intermediate in reactions of diketene and its derivatives.² Acetylketene (**2**) has recently been postulated as a reactive intermediate in the thermal decomposition of 2,2,6-

trimethyl-4*H*-1,3-dioxin-4-one (**1**), the "diketene-acetone adduct" (Scheme I).³⁻⁵ This latter postulate is supported by various empirical observations which suggest that acylketenes are generated from the thermolysis of 1,3-dioxinones⁶ and other pre-

(3) (a) Jäger, G.; Wenzelburger, J. *Liebigs Ann. Chem.* **1976**, *16*, 1689-1712. (b) Sato, M.; Kanuma, N.; Kato, T. *Chem. Pharm. Bull.* **1982**, *30*, 1315-1321. (c) Sato, M.; Ogasawara, H.; Yoshizumi, E.; Kato, T. *Chem. Pharm. Bull.* **1983**, *31*, 1902-1910.

(4) Hyatt, J. A.; Feldman, P.; Clemens, R. J. *J. Org. Chem.* **1984**, *49*, 5105-5108.

(5) Clemens, R. J.; Hyatt, J. A. *J. Org. Chem.* **1985**, *50*, 2431-2435.

(1) Correspondence may be addressed to either author.

(2) (a) Clemens, R. J. *Chem. Rev.* **1986**, *86*, 241-317, and references therein. (b) Maujean, A.; Chuche, J. *Tetrahedron Lett.* **1976**, *16*, 2905-2908.